

Synthesis, Chromatographic Purification, and Isolation of Epothilone–Folic Acid Conjugate BMS-753493

Soong-Hoon Kim,^{*,†,♦} Nuria de Mas,^{*,‡,●} Luca Parlanti,^{‡,□} Olav K. Lyngberg,[‡] Guido Ströhlein,^{¶,||} Zhenrong Guo,^{‡,■} Konstantinos Dambalas,[‡] Victor W. Rosso,[‡] Bing-Shiou Yang,^{‡,△} Kevin P. Girard,^{‡,▲} Zerene A. Manaloto,^{‡,○} Germano D'Arasmo,^{||} Riccardo E. Frigerio,^{||} Wei Wang,[§] Xujin Lu,[§] Mark S. Bolgar,[§] Madhushree Gokhale,[⊥] and Ajit B. Thakur[⊥]

[†]Oncology Discovery Chemistry, Bristol-Myers Squibb Company, Route 206 & Province Line Road, Princeton, New Jersey 08543, United States

[‡]Process Research and Development, [§]Analytical Research and Development, [⊥]Biopharmaceutics; Bristol-Myers Squibb Company, One Squibb Drive, New Brunswick, New Jersey 08901, United States

[¶]ChromaCon AG, Technoparkstrasse 1, 8005 Zurich, Switzerland

^{||}NerPharMa DS, Nerviano Medical Sciences Group, Via Pasteur 10, 20014 Nerviano, Milan, Italy

 Supporting Information

ABSTRACT: We describe the synthesis, chromatographic purification, and isolation of the epothilone–folic acid conjugate BMS-753493, an investigational new drug candidate for the treatment of cancer. The main challenges for process development were the instability of BMS-753493 in aqueous solution, the design and optimization of the preparative chromatography, and the removal of phosphate salts and water from the purified material. The operating conditions of the batch chromatographic purification were optimized using a column adsorption model. The free-salt active pharmaceutical ingredient was isolated via the precipitation of its zwitterion following a careful determination of the isolation parameters that controlled thermal and pH-related decomposition. This process enabled the manufacturing of several batches (10–30 g) of cGMP quality BMS-753493.

INTRODUCTION

The folate receptor (FR) is a cell surface receptor that is highly expressed in tumor tissues of epithelial origin while minimally expressed in normal tissues.¹ The FR binds folic acid and its conjugates tightly (dissociation constant $K_d < 10^{-9}$ M). Receptor endocytosis, dissociation, and release of the conjugate inside the cell have been demonstrated in preclinical in vitro and in vivo models. Studies with cytotoxic folic acid conjugates in cell lines and tumor models are consistent with the selective targeting of cells that overexpress the FR.² This differential tissue selectivity suggests a potential for increased therapeutic index and reduced toxicity. BMS-753493 (**1**), an epothilone–folic acid conjugate, shows preclinical efficacy consistent with the selective delivery of the cytotoxic epothilone into tissues that overexpress the FR and is an investigational new drug (IND) candidate for the treatment of cancer.³ Epothilones are cytotoxics with proven clinical efficacy.⁴ Other groups are pursuing similar FR-targeted strategies using different cytotoxics (e.g., vinblastine–folate).⁵

The dominant structural feature in compound **1** (molecular weight 1570 Da) is the highly polar peptide fragment, which has a major influence in its physicochemical properties. Additionally, **1** contains functional groups that are pH (lactone, chiral centers, carbonate, and aziridine), UV (folate), and chemically (disulfide bond) sensitive. The compound contains multiple ionizable groups, including four carboxylic acids (pK_a 3.0, 4.3, 4.4, 5.9), an aziridine (pK_a 6.6), and a guanidine (calculated $pK_a \approx 13.8$), with an isoelectric point (pI) in the range of 3.5–4.5.

The manufacturing of peptide-based active pharmaceutical ingredients (API) nearly always involves a chromatographic purification step⁶ as peptides are difficult to crystallize. In addition, the aqueous solubility of charged peptides limits the number of processing options for isolation. Understanding the transition from reaction to chromatography, developing a robust chromatographic purification, and defining the processing ranges that maintained API stability were regarded as the important issues for the development of an early-stage synthesis process of BMS-753493. We here describe a synthesis process that addresses these issues.

RESULTS AND DISCUSSION

Form Selection. During the discovery process, **1** was isolated after batch reverse-phase high-performance liquid chromatography (HPLC) as a lyophile containing sodium phosphate salts.⁷ A large variation in API content (31–81 wt %) as well as in the levels of sodium phosphate salts and water in the individual lyophile batches occurred on scale, presumably because of the variable amount of API injected per column volume (load) during the chromatographic purification and the hygroscopicity of the lyophiles.

Before undertaking process optimization, API form evaluation studies were initiated to identify the form that offered minimal

Received: February 1, 2011

Published: May 03, 2011

Table 1. Stability data of the sodium salt of **1** in aqueous solution (pH 7.0) at -70 , -20 , and 5 °C

temp. (°C)	time	number of freeze/thaw cycles	potency (mg/mL) ^a	HPLC purity at 250 nm (area percentage [AP])
-70	initial	none	10.2	97.93
	1 week	1	10.8	97.87
	20 weeks	8	10.4	97.50
	24 weeks	9	10.5	97.48
	26 weeks	1	10.2	97.65
-20	initial	1	10.5	98.00
	1 week	4	10.3	97.86
	4 weeks	6	10.9	97.45
	15 weeks	8	10.1	97.16
5	initial	1	10.7	97.99
	4 h	2	10.8	97.79
	48 h	4	10.5	97.31
	1 week	4	10.6	96.11

^aThe method precision for sample repeatability (RSD) is $\leq 2.5\%$. The variation in potency at -70 °C, RSD 2.4%, is thus not significant.

batch-to-batch variability in potency as well as the highest stability and processing flexibility for subsequent API formulation studies. No crystalline forms of **1** were found through high-throughput screening of counterions (Mg^{2+} , Zn^{2+} , Ca^{2+} , Tris^+ , K^+ , and others) at pH 2–9 using the antisolvents methanol, ethanol, acetone, and THF. Stability studies of amorphous lyophiles prepared at pH 7 using different counterions demonstrated that the salts were highly hygroscopic (10–15 wt % moisture uptake at 40–50% relative humidity).

The sodium and potassium salts exhibited comparable superior solid stability than the calcium and magnesium salts as well as the zwitterion (ZI) but were prone to hydrolysis unless stored under subzero temperatures. Because neither of these salts could be prepared in crystalline form, isolation required a lyophilization step. Stringent storage restrictions would have been required to maintain constant moisture content in these highly hygroscopic solids. In addition, lyophilization was challenging to implement for the production of bulk API because of the electrostatic, highly active nature of the lyophilized solid. Similarly, the stability of the sodium salt in aqueous solution at pH 7.0 was acceptable only at subzero temperatures (Table 1), with -70 °C giving the best stability over 26 weeks. As the aqueous solution was an acceptable form because **1** is administered intravenously, these findings led to the selection of the sodium salt as a 10–15 mg/mL solution at pH 7.0⁸ stored at -70 °C as the API. All further work was focused on producing this solution as the final product.

The sodium salt of **1** in aqueous solution has only modest stability at room temperature: its half-life at pH 7 is 11 days, and it undergoes 82% degradation at pH 9.5 after 24 h. The selection of sodium over potassium as the counterion during the reaction avoided a salt-exchange step to sodium during isolation. Note that the mobile phase of the HPLC purification also contained sodium.

Limitations of the Discovery Process and Goals for Process Improvements. The discovery process (up to 1 g of **1**) included steps that were not easily scalable. The synthesis of the API involved the exchange of a cysteine thiol **2** with an activated

disulfide **3** (Scheme 1). The reaction in THF/aqueous NaHCO_3 was heterogeneous, and the impure API solids were separated using centrifugation. THF was removed by distillation, and the resulting solution was passed through a $1\text{-}\mu\text{m}$ filter and purified by preparative reverse-phase HPLC ($\text{NaH}_2\text{PO}_4/\text{Na}_2\text{HPO}_4$ and acetonitrile). Acetonitrile was removed from the API fractions by distillation, and the solution was lyophilized. A second chromatography with water/acetonitrile to remove the phosphate salts was followed by yet a second lyophilization to isolate **1** as a lyophile.⁹

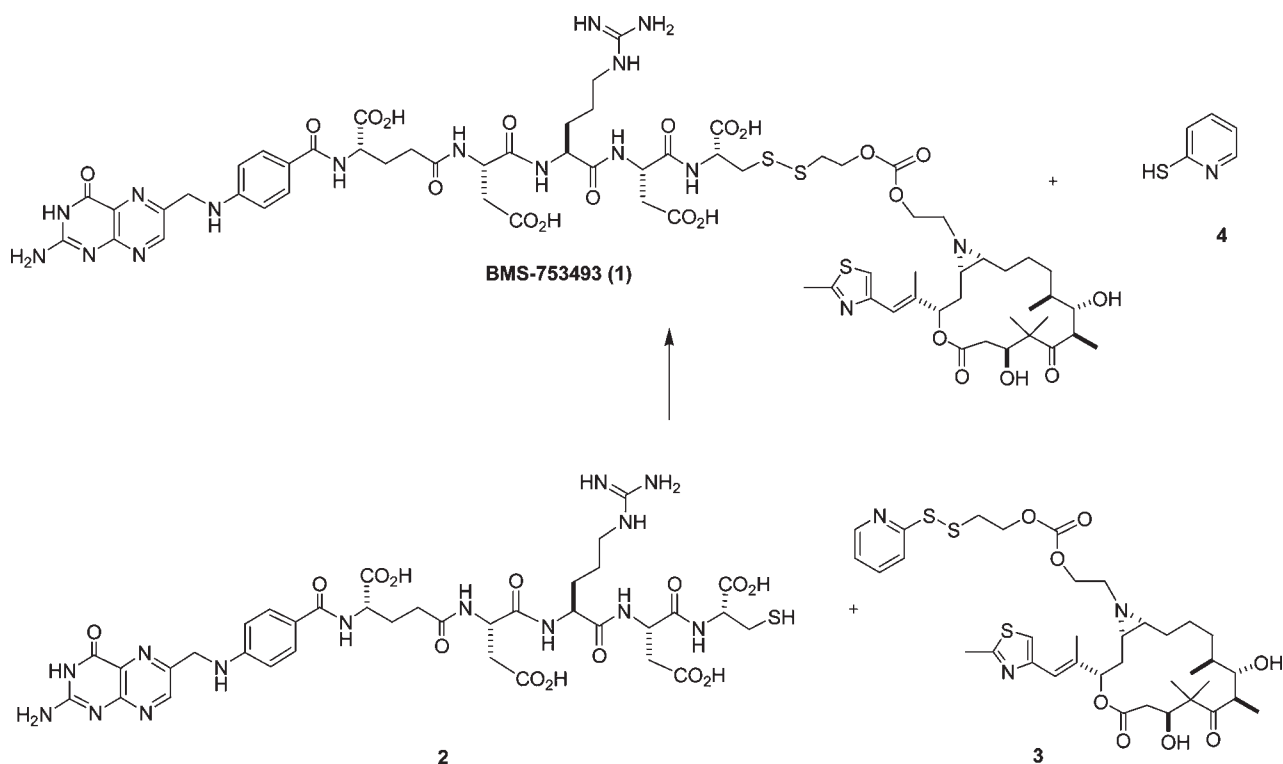
Such a process possessed several challenges. Solids were removed from the reaction mixture by centrifugation because filtration was unacceptably slow. Only the supernatant was processed further; however, API remained in the pellet, reducing the yield. The poor thermal stability of the API required avoiding the high-temperature distillation of water (2% API degradation at 30 °C in 6 h in the concentration range 1.2–5.9 g/L). A second chromatography was required to obtain the salt-free final API solution. In addition, **1** is a potent cytotoxic agent that was handled using the highest level of engineering controls in specialized containment scale-up facilities, underscoring the need for a more streamlined process.¹⁰ Strategically, we viewed the IND toxicology campaign (5 g, 3 mmol) as an opportunity to define an alternate synthesis strategy with process controls, to generate process knowledge, and to define processing ranges that maintained API stability. The first cGMP campaign (>10 g of **1**) was subsequently used to define the scalability limits of this new synthesis process with stricter requirements for purity.

Process Development. To initiate our studies, the relationship between stoichiometry and reaction outcome (product distribution, relative reaction rates) was examined (Table 2). The reaction followed a simple profile: excess of reagent **3** consumed its counterpart **2** and vice versa, and no significant side products were observed. A small amount of oxidative dimerization of peptide **2** ($<5\%$ of symmetrical disulfide dimer) was observed in all cases. Because peptide **2** was available from a custom commercial supplier, epothilone **3** (available in 10 steps from the natural product epothilone A in 12% overall yield) was used as the limiting reagent.¹¹

We explored other organic cosolvents in an attempt to maintain homogeneity of the reaction crude before transitioning to the chromatography (Table 3). The reaction mixture was homogeneous using methanol (entry 3) with an acceptable reaction rate. Moreover, up to 40 vol % of methanol in the reaction mixture did not appreciably change the shape or the resolution of the BMS-753493 peak in the HPLC trace from its closest eluting impurities during chromatographic purification. Methanol was thus selected as the cosolvent, and the crude reaction mixture was used directly as the feed for the chromatography.

Transition to Chromatography. A requirement for the feed of the chromatographic purification was a homogeneous and chemically stable reaction crude. Table 4 shows the feed stability (criteria: visual inspection for homogeneity and HPLC for purity) versus time and temperature. Only a mixture at 22 °C after 8 days produced turbidity; all other observations were clear. We found that the major determinant for homogeneity of the reaction crude was maintaining the pH at <6.5 by charging 1 N HCl. If this threshold was not breached, the crude was homogeneous at 4 °C for 24 h and at -24 °C for 8 days. A $1\text{-}\mu\text{m}$ filtration was performed, and the solution was ready for separation. The $\text{Na}_2\text{HPO}_4/\text{NaH}_2\text{PO}_4$ buffer gave a more consistent reaction crude pH after quenching and a smaller drift toward

Scheme 1. BMS-753493, an eptothilone–folic acid conjugate

Table 2. Effect of excess reagent on reaction profile^a

entry	excess	composition of reaction crude quenched after 180 min (HPLC AP at 278 nm) ^b			
		product 1	peptide 2	epothilone 3	pyridine 4
1	none	66.8	7.4	4.4	20.5
2	1.5 equiv of 2	65.8	13.0	<1	21.1
3	1.5 equiv of 3	68.0	2.8	6.1	17.5

^a Reaction conditions: 21 mg of 3 (0.01 M); 50/50 vol % THF/aqueous NaHCO₃ (0.06 M); room temperature; quenched with 7 mM Na₂HPO_{4(aq)}, pH 7.2 (50/50 vol % reaction mixture/quenching solution). ^b All impurities resolved by the HPLC method were integrated, but not all APs are shown.

higher pH over time compared with NaHCO₃. The stability of reaction crudes containing Na₂HPO₄ showed a similar behavior as those containing NaHCO₃: homogeneous, stable solutions were obtained at 4 °C and −24 °C for at least 3 days at pH 6.3.

Chromatographic Purification. The chromatographic purification of 1 was performed using batch mode on a column with an internal diameter of 8 cm because only 100 g of API were required for the clinical studies up to phase II. Batch chromatography also afforded flexibility during development as process parameters could be adjusted to enable the purification of reaction crudes of variable quality. The objectives of the chromatographic purification development were to define a protocol that separated BMS-753493 from the excess peptide 2, mercaptopyridine byproduct 4, and one unidentified peptide-related isomeric impurity 5 that eluted on the compressive front of the main peak (Figure 1). The polymeric resin Amberchrom HPR10 (polystyrene/divinylbenzene,

Table 3. Effect of solvent on initial conversion to 1^a

entry	solvent	composition of reaction crude quenched after 5 min (HPLC AP at 278 nm) ^b			
		product 1	peptide 2	epothilone 3	pyridine 4
1	THF	32.8	50.1	7.0	10.1
2	acetonitrile	67.7	1.2	3.7	23.3
3	methanol	71.1	<1.0	2.2	25.6
4	DMF ^c	67.3	<1.0	1.5	23.5

^a Reaction conditions: 5 mg of 3 (0.01 M), 1 equiv of 2; 50/50 vol % cosolvent/aqueous NaHCO₃ (0.06 M); room temperature; quenched with 7 mM Na₂HPO_{4(aq)}, pH 7.2 (50/50 vol % reaction mixture/quenching solution). ^b All impurities resolved by the HPLC method were integrated, but not all APs are shown. ^c DMF has AP of 5.8.

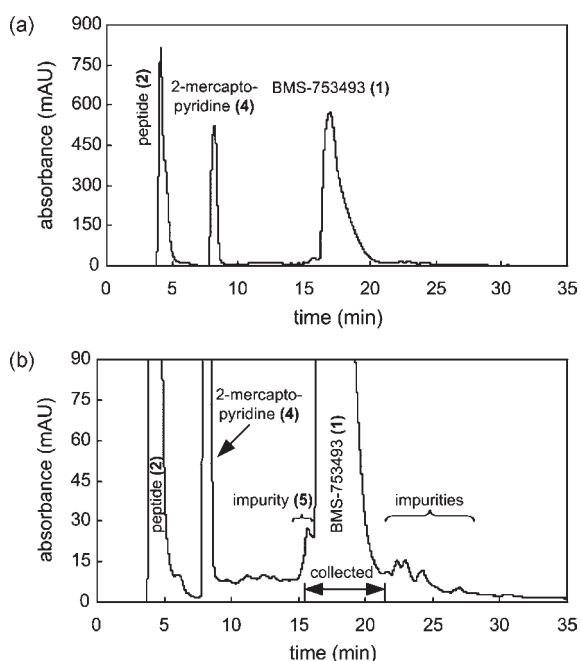
10 μm, 300 Å) was selected over a traditional silica-based hydrophobic resin for its ability to withstand strongly basic treatments (pH 14) for cleaning and depyrogenating the resin in place.

A gradient method was initially selected to eliminate variability in retention times caused by slight differences in the composition of the mobile phase and to ensure process robustness. Although an isocratic method (84/16 vol % A/B)¹² offered an analytical separation comparable to that of the gradient method, it required controlling the composition of the mobile phase within 0.5% to obtain reproducible retention times, a range that was difficult to achieve consistently on scale.¹³ The recovery of BMS-753493 through the elution was nearly quantitative (98%).¹⁴ The impurity profiles of the reaction crude and a representative API sample purified by preparative HPLC are shown in Table 5.

Table 4. Stability of the reaction crude versus time and temperature^a

entry	temp. (°C)	time = 0	API HPLC purity at 278 nm (AP)		
			1 day	4 days	8 days
1	22	57.4	58.4	42.3	38.7 ^b
2	4	57.4	59.8	48.6	51.0
3	-24	57.4	54.8	58.2	54.0

^a Reaction conditions: 30 mg of **3** (0.01 M), 1.4 equiv of **2**; 50/50 vol % methanol/aqueous NaHCO₃ (0.06 M); room temperature; quenched after 90 min with 7 mM Na₂HPO_{4(aq)}, pH 7.2 (66/33 vol % reaction mixture/quenching solution); pH after quenching 6.4. At time = 0, AP of **2** = 18.7, AP of **4** = 23.1, homogeneous solution. ^b Only this solution was no longer clear.

**Figure 1.** Preparative chromatogram of the reaction crude using the initial purification method. Load = 1.1 g/L column.

The API isomeric impurity **5**, derived from an isomer present in the peptide **2**, was the most difficult impurity to purge. The ability to separate this particular impurity defined our criterion for acceptable purity, and only fractions that produced <0.50 AP (250 nm) upon pooling were selected.

The width of the API preparative peak increased by 10% when the load doubled from 0.6 g/L to 1.2 g/L (Table 6). Consequently, the API amount loaded per injection (not its concentration) primarily determined the elution volume to process through the isolation. Note that the load was increased from 1.0 to 2.1 g/L from the development runs (5 cm × 25 cm prepacked column or column with dynamic axial compression, DAC) to the cGMP campaign (8 cm × 30 cm DAC column). A representative API preparative peak at production scale is shown in Figure 2. Pooled fractions were held at -24 °C or -70 °C for several days before isolation (Table 7).

The level of the isomeric impurity **5** in the reaction crude varied depending on the initial quality of the peptide **2**. This daughter impurity was partially separated by the initial purification method, causing variability in the purification yield (Table 8). We found

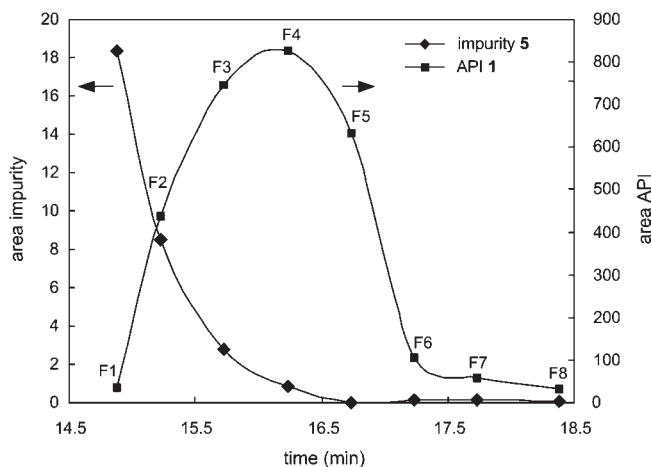
Table 5. Impurity profiles of representative reaction crude and isolated API purified by reverse-phase batch preparative HPLC

sample	HPLC purity at 250 nm (AP)						
	relative retention time (RRT) (-) ^a						
	0.37	0.96	1.00	1.06	1.08	1.11	1.44
crude	0.52	0.63	78.59	0.00	0.00	0.51	0.36
isolated API	0.08	0.30	99.58	0.03	0.00	0.07	0.07
specification	0.79	0.50	97.0	0.65	0.50	0.50	0.73

^a Retention time of key impurities, i.e., relevant to the chromatographic purification, relative to that of the API on the HPLC analytical method. The RRTs of API degradants are 0.37, 1.11, and 1.44. The RRTs of API isomers are 0.96 (**5**, daughter impurity of isomeric impurity in peptide **2**), 1.06, and 1.08. The impurity **5** is controlled through the chromatographic purification (its level does not increase during the API isolation).

Table 6. Width of the API preparative peak as a function of load using the initial purification method (0.46 cm × 25 cm, 0.7 mL/min)

[API] in crude (mg/mL)	load (mg)	load (g/L column)	peak start (min)	peak end (min)	peak width (min)
4.7	2.3	0.6	16.9	21.3	4.4
13.7	2.5	0.6	16.7	21.3	4.6
20.5	2.5	0.6	16.5	21.5	5.0
4.7	2.3	0.6	16.8	21.3	4.5
4.7	5.0	1.2	16.4	21.4	5.0
20.5	4.6	1.1	16.1	21.2	5.1

**Figure 2.** Preparative API peak using the initial purification method at production scale (8 cm × 30 cm, 132 mL/min). Load = 1.9 g/L column. The peak was cut into eight fractions (F1–8) to monitor the impurity **5**.

that when the level of the parent isomeric impurity in **2** was 1 AP, the entire API preparative peak could be collected (Figure 1b) to meet the desired specifications (<0.50 AP of impurity **5** in the product). However, at 2–3 AP levels, the quantity of **5** reached an unacceptable 0.9–1.0 AP in the product if the entire API peak was collected. As the impurity was not distributed uniformly over the

Table 7. Stability of the pooled fractions after chromatographic purification, defined as the time at which the API HPLC purity is 0.5 AP lower than its initial purity^a

sample	temp. (°C)	HPLC purity at 250 nm (AP)	stability
1	22	97.5	<24 h ^b
2	-24	97.7	≥ 8 days
3	-70	98.2	≥ 8 days

^a Initial HPLC purity = 98.2 AP. Concentration of acetonitrile is ~20 vol % in 7 mM aqueous Na₂HPO₄, pH 7.2. ^b The stability of the pooled fractions at 22 °C is 8–10 h and at 5 °C is ≥ 24 h.

Table 8. Effect of reaction crude quality on purification yield

AP of peptide 2 isomer ^a	AP of API isomer 5 ^b	purification yield (%) ^c
1.0	<0.50	98
2.1	0.85–0.90	77–93
3.0	0.97	75

^a Parent impurity of impurity 5. ^b Calculated for the impurities that partially coelute with the API during the chromatographic purification (RRT 0.96, 1.06, 1.08, and 1.11 on the HPLC analytical method). Typical crude HPLC purity = 80.5 AP. ^c Using the initial purification method to achieve <0.50 AP of 5 in the pooled fractions.

API peak, our initial approach to controlling this impurity was by fractionating the peak and analyzing for the impurity (Figure 2). Any early fractions that resulted in >0.50 AP of 5 in the purified pool were set aside for later recovery.

Model-Based Purification of Mixed Fractions. While our initial purification method operated efficiently, a significant quantity of API remained mixed with the impurity 5 at >0.50 AP levels. A viable and cost-effective purification process would be needed to harvest this product. A modeling approach was explored to obtain process parameters for the purification of such fractions.¹⁵ The objectives were to maximize the overall purification yield while still fitting the purified solutions into the 2.5-L dedicated isolation vessel in our facility. Model-based guidelines were used to design the purification and isolation strategy. This information would have been difficult to obtain experimentally through a statistical design of experiments and would have required API amounts and analytical resources that were not readily available. The model was constructed by using only a small amount of material (~150 mg), a small number of experiments (5), and minimal separation work (2 runs with fractionation, analysis of 22 samples and 4 standards).

Batch-Elution Model. It has been shown that a lumped kinetic model generally gives sufficient accuracy to model reverse-phase chromatographic purifications of peptides.¹⁶ The various mass transfer components, i.e., film diffusion, pore diffusion, and adsorption kinetics, are lumped into a single resistance. The governing partial differential equations are

$$\varepsilon^* \frac{\partial c_i}{\partial t} + (1 - \varepsilon^*) \frac{\partial q_i}{\partial t} + u_{sf} \frac{\partial c_i}{\partial z} = D_{eff} \frac{\partial^2 c_i}{\partial z^2} \quad (1)$$

$$\frac{\partial q_i}{\partial t} = k_m (q_i^{eq} - q_i) \quad (2)$$

where eq 1 is the component mass balance in the liquid phase and eq 2 is the mass transfer equation.¹⁶ The variables c_i and q_i are the concentrations of component i in the liquid and solid phases,

Table 9. Parameters used in the batch-elution model for the API 1 and the impurity 5

parameter	value
ε^* (-)	4×10^{-1}
k_m (1/min)	9×10^1
d_{ax} (cm)	5×10^{-3}
number of axial discretization points	4×10^2

respectively; t is the time; z is the axial coordinate; ε^* is the total porosity; u_{sf} is the superficial flow velocity (volumetric flow rate divided by column cross sectional area); k_m is the lumped solid–liquid mass transfer coefficient; $D_{eff} = u_{sf} \times d_{ax}$ is the effective axial dispersion coefficient; and d_{ax} is the reduced axial dispersion coefficient. The solid-phase concentration in equilibrium with c_i is q_i^{eq} , which is given by the adsorption isotherm. A bi-Langmuir adsorption isotherm was used, where c_M is the concentration of the modifier (acetonitrile), and α_1 – α_8 are the component-dependent isotherm parameters. Equations 1, 2, and 3a–3f were solved numerically using appropriate initial and boundary conditions¹⁶ and the parameter values shown in Table 9. The experimental conditions used in this modeling study are shown in Table 10.

$$q_i^{eq} = \frac{c_i H_{I,i} + q_{I,i}^{\infty} \Omega_{I,i}}{1 + \sum_j \left(\frac{C_j H_{I,j}}{q_{I,j}^{\infty}} + \Omega_{I,j} \right)} + \frac{c_i H_{II,i} + q_{II,i}^{\infty} \Omega_{II,i}}{1 + \sum_j \left(\frac{C_j H_{II,j}}{q_{II,j}^{\infty}} + \Omega_{II,j} \right)} \quad (3a)$$

$$H_i = \alpha_{1,i} (C_M)^{\alpha_{2,i}} \quad (3b)$$

$$H_{II,i} = \alpha_{3,i} (H_i)^{\alpha_{4,i}} \quad (3c)$$

$$H_{I,i} = H_i - H_{II,i} \quad (3d)$$

$$q_{I,i}^{\infty} = \frac{\alpha_{5,i} H_{I,i}}{1 + \frac{\alpha_{5,i}}{\alpha_{6,i}} H_{I,i}} \quad (3e)$$

$$q_{II,i}^{\infty} = \frac{\alpha_{7,i} H_{II,i}}{1 + \frac{\alpha_{7,i}}{\alpha_{8,i}} H_{II,i}} \quad (3f)$$

First, using the fitted Henry functions H_i , i.e., α_1 and α_2 , and a set of estimated nonlinear isotherm parameters α_3 – α_8 , simulations for BMS-753493 were carried out for several overloaded runs on an analytical column (0.46 cm × 25 cm, loads 0.6–2.0 g/L) as well as on a preparative column (8 cm × 30 cm, loads 0.7–2.2 g/L). The resulting chromatograms showed reasonable agreement with the experimental peak shapes (Figure 3). This may be partly attributed to the structure of the adsorption-isotherm equations, where all nonlinearities are scaled only with the Henry coefficient of the compound studied. The deviation in the peak retention times observed between experiments and simulation was attributed to a systematic offset between the experimental and simulated concentrations of acetonitrile. The measured Henry function was assumed to be accurate, thus the concentration of acetonitrile in the simulation input was adjusted by a constant factor so that the experimental and simulated peak

tails overlapped. Second, the isotherm parameters α_3 – α_8 were fitted by minimizing the error between the experiments carried out on the analytical column and the corresponding simulation. The experimental data from the preparative column were not used for this fitting procedure because their reliability was unclear. The results of this fitting procedure are shown in Figure 4, and the fitted

Table 10. Operating conditions of the chromatographic purification of the API 1 used for the modeling study

experiment	method	column diameter (cm) × length (cm)	flow rate (mL/min)	load (g/L)
1	10–50% B in 30 min	2.2 × 25	10	2.8
2	10–50% B in 30 min	8.0 × 30	132	7.2 × 10 ⁻¹
3	10–50% B in 30 min	8.0 × 30	132	2.0
4	10–50% B in 30 min	8.0 × 30	132	7.9 × 10 ⁻¹
5	10–50% B in 30 min	8.0 × 30	132	8.7 × 10 ⁻²
6	10–50% B in 30 min	8.0 × 30	132	2.2
7	10–50% B in 30 min	0.46 × 25	1	2.0
8	10–50% B in 30 min	0.46 × 25	1	5.6 × 10 ⁻¹
9	10–50% B in 30 min	0.46 × 25	1	5.6 × 10 ⁻¹
10	10–50% B in 30 min	0.46 × 25	1	9.9 × 10 ⁻¹
11	10–50% B in 30 min	1.0 × 25	5	7.9 × 10 ⁻¹
12	16% B isocratic	0.46 × 25	1	2.7 × 10 ⁻²
13	18% B isocratic	0.46 × 25	1	2.7 × 10 ⁻²
14	20% B isocratic	0.46 × 25	1	2.7 × 10 ⁻²

values of α_3 – α_8 are shown in Table 11. The agreement between experimental and simulation was satisfactory.¹⁷

Next, using the fitted parameters α_3 – α_8 , simulations for the API 1 and the impurity 5 were carried out for several cGMP runs (8 cm × 30 cm), where the load was increased from 0.7 to 2.8 g/L (Figure 5). The agreement between the experimental and simulated profiles of 1 became inaccurate with increasing loads (≥ 2 g/L, experiments 1, 3, 6). The agreement for the impurity was inaccurate primarily because of the poor simulation of the peak shape of 1.

To explain the deviation between the experimental and simulated peak shapes for the cGMP runs, we postulated that the buffering strength of the mobile phase was insufficient to keep the pH constant at high API concentrations. The aqueous buffer pH is 7.2. A typical pH of the pooled fractions after acetonitrile removal, however, was around 6.5 (load 2.0 g/L), thus below the buffer pH. High API concentrations would locally change the pH during the elution, which in turn would necessitate a change in the charge of the API. The charge of the API may change in the pH range 6.5–7.2 because the pK_a of the aziridine is 6.6. By increasing the buffering strength of the mobile phase (70 mM Na₂HPO₄), Langmuir peak shapes were obtained for loads of up to 3 g/L.

Large-Scale Purification of Mixed Fractions. The batch-elution model was then used to select operating conditions with higher load and product purity. The elution volume was not used as a constraint in the optimization. These optimized conditions were verified experimentally (Table 12); the load was increased from 2.6 to 3.7 g/L although the yield predicted by the model (90%)

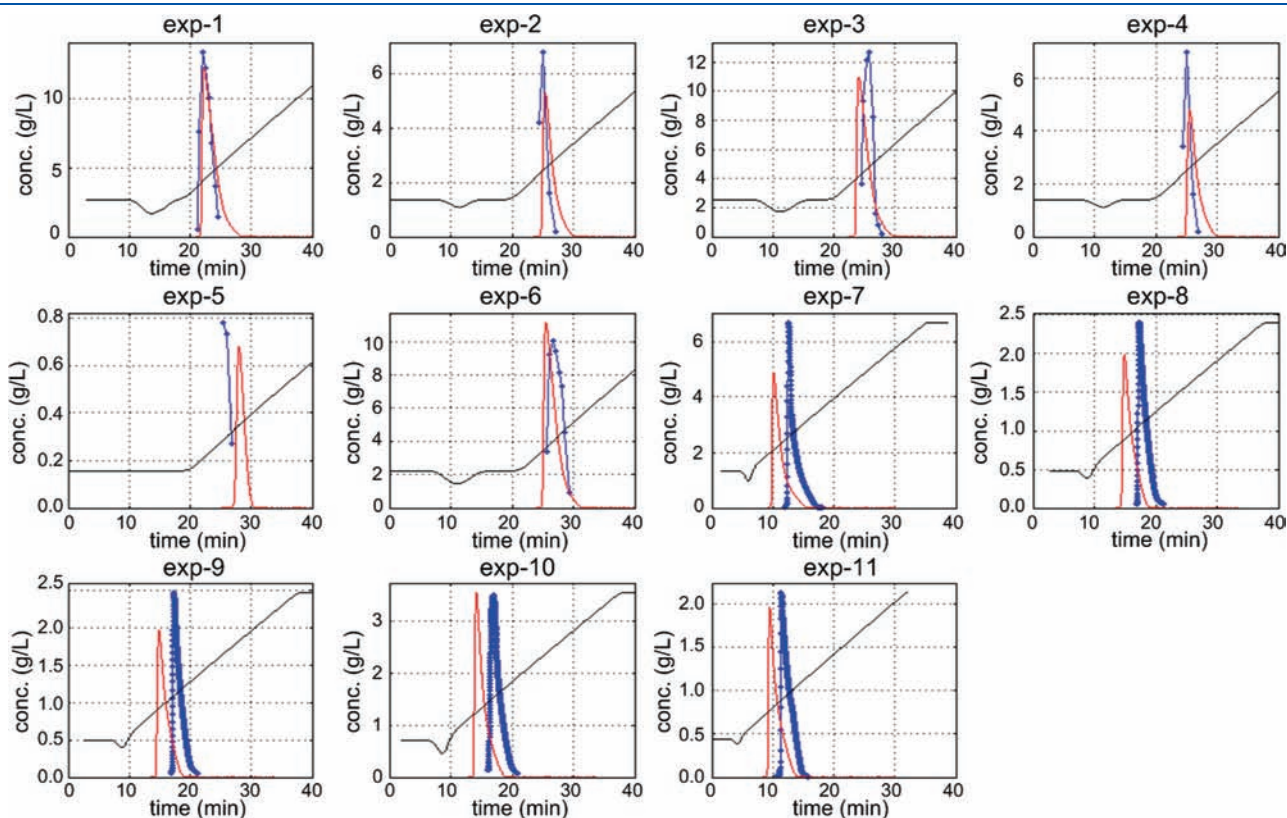


Figure 3. Simulation (red line) and experimental data (blue dots and line) for chromatograms at various operating conditions. The simulation used the measured Henry coefficient and an initial set of estimated nonlinear isotherm parameters α_3 – α_8 (no fitting). Black line indicates normalized, simulated acetonitrile concentration at column outlet.

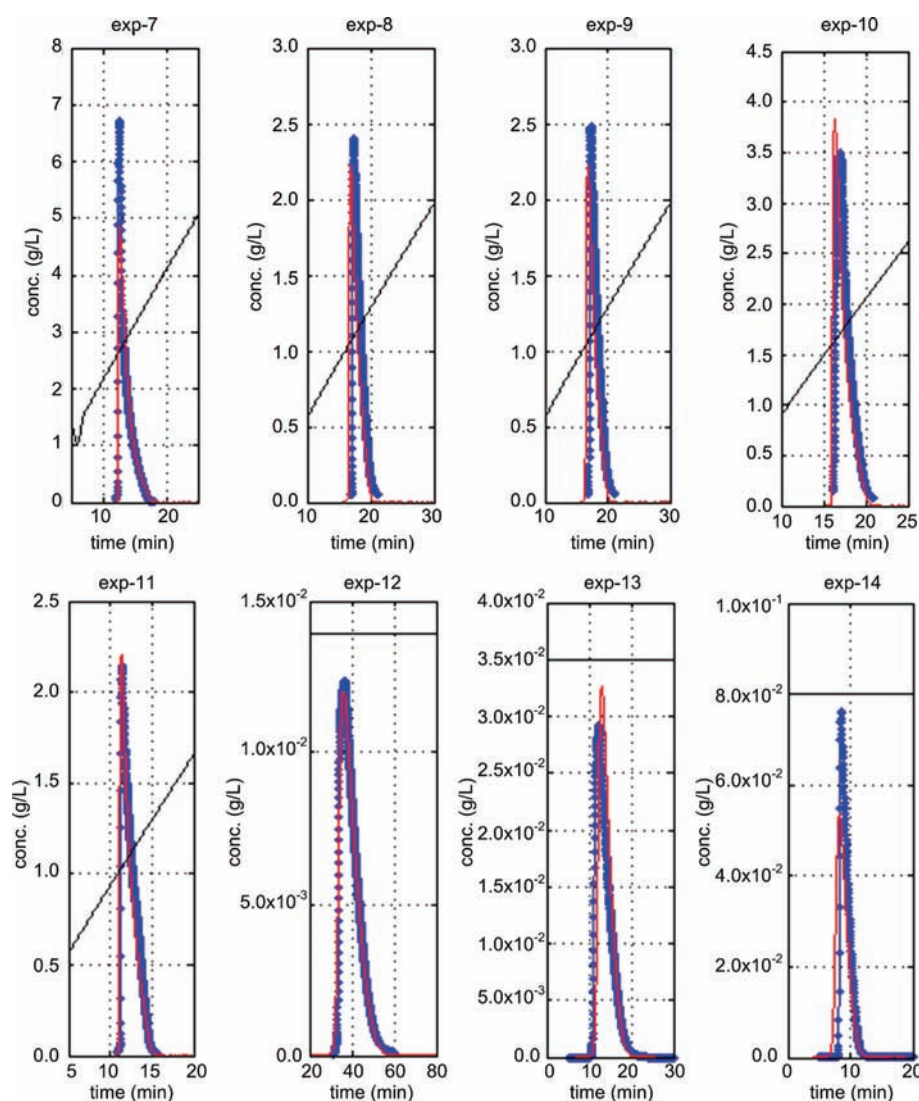


Figure 4. Simulation (red line) and experimental data (blue dots and line) for chromatograms at various operating conditions, excluding cGMP runs. The simulation used the measured Henry coefficient, fitted nonlinear isotherm parameters α_3 – α_8 , and concentrations of acetonitrile adjusted by approximately $\pm 5\%$. Black line indicates normalized, simulated acetonitrile concentration at column outlet.

Table 11. Fitted isotherm parameters α , for the API 1 and the impurity 5

parameter	API 1	impurity 5
α_1	1.940×10^{18}	2.054×10^{17}
α_2	−8.104	−7.698
α_3	3.55×10^{-1}	3.55×10^{-1}
α_4	7.66×10^{-1}	7.66×10^{-1}
α_5	2.0×10^{-1}	2.0×10^{-1}
α_6	6.0	6.0
α_7	1.0×10^4	1.0×10^4
α_8	1.8×10^2	1.8×10^2

was not achieved. Next, the model was used to evaluate qualitatively the impact of the level of the impurity 5 in the reaction crude on the purification yield at different loads (Figure 6). For an impurity level of 1%, the yield was 85% and independent of the load. At 5%, the yield dropped to 65% and further down to 42% when the load

reached >4 g/L. For a level of 10%, the best yields of $\sim 45\%$ were obtained at intermediate loads of 1.8–3.7 g/L. Such loads displayed the lowest yield decrease when the impurity level increased in the crude: $\sim 5\%$ yield was lost per every additional percent of impurity in the crude.

These guidelines were used to group the mixed fractions into five sets according to the level of the impurity 5 (Table 13). Fractions containing >12 AP of 5 were discarded outright. These sets were then pooled into two groups for purification using either the initial method or the model-based method. The latter method was implemented to purify 4.7 g of API 1 containing 7.8 AP of the impurity 5 on scale (8 cm \times 30 cm column, 132 mL/min, load 3.8 g/L), with a purification yield of 56%, which was consistent with the model prediction. The addition of this API to the quantities purified in the initial chromatography negated the need to initiate a new, costly API production campaign from epothilone A.

Isolation. Following purification, the remaining unit operations consisted of the removal of acetonitrile, phosphate salts, and

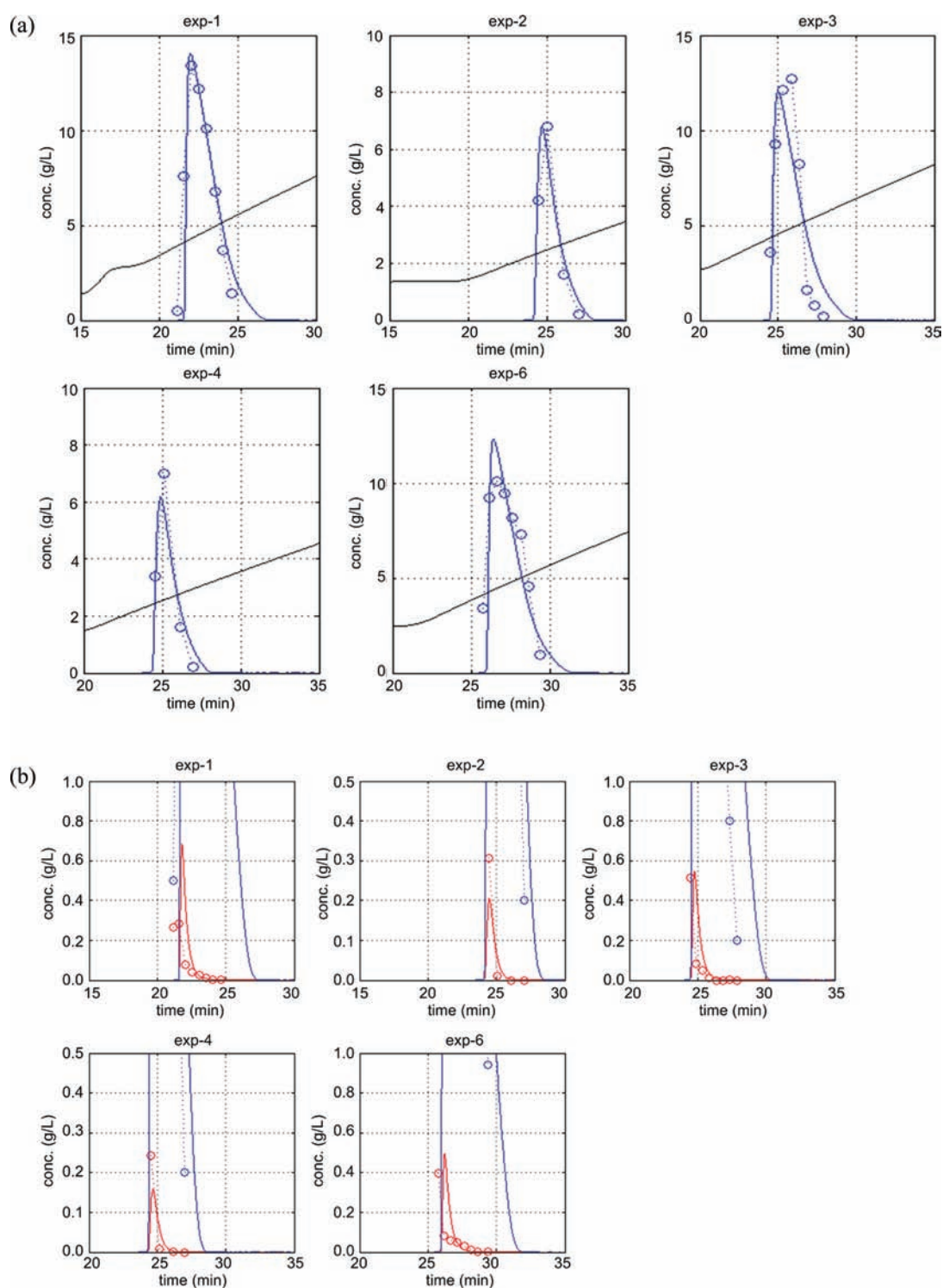


Figure 5. Simulation after isotherm-parameter fitting (line) and experimental data (marker) for various cGMP runs: (a, b) API 1 (blue), (b) impurity 5 (red). The cGMP runs were not used to fit the isotherm parameters. Black line indicates normalized, simulated acetonitrile concentration at column outlet.

water to isolate the API as a salt-free aqueous solution. In the discovery process, acetonitrile was distilled, and the pooled fractions were lyophilized. The lyophilized API contained a mixture of sodium phosphate salts (9 wt %) and water (12 wt %). Alternatively, the pooled fractions were desalted using a second chromatography (water/acetonitrile) and lyophilized. As a reference, a 10-g input of ephedrine 3 was estimated to generate 10 L

of aqueous product solution, which would have required tedious lyophilization. Instead, we instituted an alternate strategy that avoided lyophilization and reduced processing time.

While the formation of an insoluble zwitterion via pH control is commonly employed for the isolation of charged peptides,^{6c} BMS-753493 contains several pH sensitive moieties, so the validity of pH control needed to be determined. ZIs of BMS-753493

with various counterions had been evaluated earlier as potential forms of the drug substance but were found to be too unstable for long-term storage and handling. Nevertheless, we revisited the formation of an insoluble ZI as a process intermediate because it would potentially simplify the isolation by allowing the removal of both phosphate salts and water via filtration in a single step. In this new context, the process design objectives were to minimize the API losses in the filtrate and to define the processing ranges that maintained ZI stability.

Table 12. Experimental results for the initial and model-based purification methods^a

	initial method ^b	model-based method ^c
load (g API 1/L column)	2.6	3.7
gradient slope (g acetonitrile/L mobile phase/min)	10.5	1.0
purification yield (%)	83.9	84.7
purity of pooled fractions (AP)	99.2	99.6
level of impurity 5 in crude (AP)	0.95	0.95
level of impurity 5 in pooled fractions (AP)	0.33	0.27

^a A = 7 mM Na₂HPO₄, pH 7.2; B = acetonitrile (0.46 cm × 25 cm, 0.5 mL/min). ^b 10–50% B in 30 min. ^c 9.3–20.8% B in 90 min, gradient shifted by a system suitability test (SST) (–2% B).¹⁸

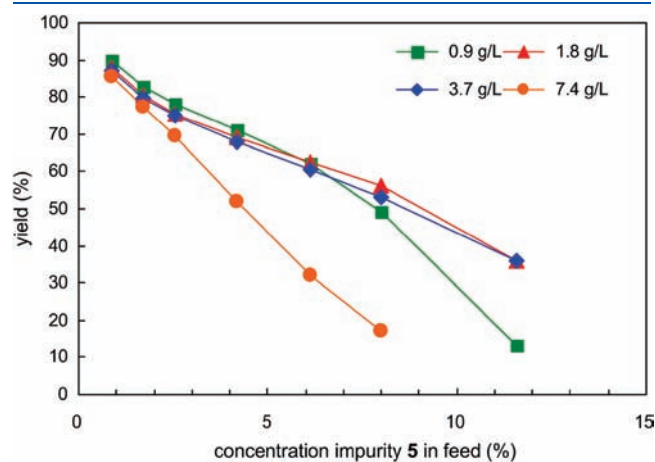


Figure 6. Purification yield as a function of the level of the impurity 5 in the reaction crude and load using the model-based purification method. Purity of product pool: 99.7%.

Table 13. Experimental results for the model-based purification of mixed fractions

set #	HPLC purity (AP of 5 unless otherwise noted)	input		preparative method	expected yield (%)	expected amount of 1 (g)	actual amount of 1 (g)	
		batch #	amount of 1 (g)					
1	<0.50	1, 2	1.7	initial	100	1.7	12.2	
2	0.50–3.0	1–4	13.5	(sets 1, 2)	70	9.4		
3	3.0–8.0	1–3	1.8	model-based	60	1.1	3.1	
4	8.0–12.0	2–4	2.9	(sets 3–5)	45	1.3		
5	4.0 ^a	2, 3	0.8		90	0.7		
			total: 20.7				total: 14.2	total: 15.3

^a Degradants due to thermal decomposition.

The isoelectric point of BMS-753493 in water was between pH 3.5–4.3, as measured by its lowest solubility value.¹⁹ The ZI could be formed using a buffer (e.g.; citric acid) or directly using dilute HCl to adjust the pH. The ZI was collected by filtration, resuspended in water, and redissolved by neutralization to pH 7 using 0.1 N NaOH.²⁰ During base addition, the pH was kept below 7.5 to minimize the chance of degradation by brief excursions to high pH. The reconstituted solution had the desired API concentration of 10–15 mg/mL. To minimize the API losses during the ZI collection, we sought to determine the relationship between the acetonitrile and API concentrations in the purified pooled fractions and ZI solubility. The API concentration before acetonitrile distillation using the initial purification method and optimized loads (2 g/L) was ~7.5 mg/mL (Figure 2).

ZI formation directly from pooled fractions without acetonitrile distillation (Table 14, entry 1, ~20 vol % acetonitrile) showed higher API concentration in the filtrate than if distilled (entry 2, <1 vol % acetonitrile). On the other hand, ZI solubility was independent of the API concentration, ~0.05 mg/mL (entries 2–5); therefore, the API losses in the filtrate were proportional to the filtrate volume. The API concentration in entry 2 was at the lower bound of the API concentration in the pooled fractions.²¹ Thus, ZI formation proceeded with minimal API losses (<1% for the initial purification method at loads of ≥2 g/L) following acetonitrile distillation. A concentration of 2.4 vol % acetonitrile after distillation gave a comparable ZI solubility of ~0.05 mg/mL (entry 6), and it thus was selected as the end point of the distillation.²²

A homogeneous, stable reaction crude as the feed to the chromatography, a robust chromatographic purification, and the formation/filtration of the ZI to remove both phosphate salts and

Table 14. Zwitterion solubility versus API concentration in the pooled fractions after acetonitrile distillation^a

entry	initial [API] (mg/mL) ^b	[API] in filtrate (mg/mL)	API losses in filtrate (%)	yield isolated API (%) ^c
1 ^d	1.6	0.35	not available (NA)	NA
2	1.6	0.05	5	95
3	2.5	0.05	2	NA
4	5.0	0.03	0.7	98
5	5.9	0.04	0.7	NA
6 ^e	1.8	0.05	NA	NA

^a Reactions using 50 mg of 3 unless otherwise noted. ^b 0.002 vol % acetonitrile unless otherwise noted. ^c From pooled fractions (after acetonitrile distillation) to final API solution. ^d Undistilled pooled fractions (~20 vol % acetonitrile). ^e Reaction using 200 mg of 3; 2.4 vol % acetonitrile remained after distillation.

water were the key features of the new process. Importantly, the unit operations following the reaction — chromatography, distillation, filtration, and reconstitution — were amenable to control and scalable in a predictable way. This aspect was critical for process development because the API stability set the upper bound of the allowable processing time. While the ZI solid was unstable (<2 h at room temperature and 8 h at 5 °C, Table 15), the pooled fractions were stable at room temperature for ~10 h and at 5 °C for 24 h.

During the IND toxicology campaign, the isolation steps were carried out at room temperature. This protocol was not scalable beyond ~1 g as the ZI formation, filtration, and reconstitution required ~3 h at 1.5-g scale (Table 16), after which decomposition levels became unacceptable. We viewed the first cGMP campaign as an opportunity to expand the processing window to 5 °C and to possibly define the limit of the ZI isolation process. The lowest pressure available for distillation in our organics pilot plant was 25–30 mbar, and it was desirable to complete the ZI isolation within a work day of 8–10 h. This isolation procedure consisted of acetonitrile distillation at ~25 mbar and 5 °C for 4 h to attain ~10 vol % acetonitrile and further distillation at room temperature for another 2 h to reach ~2 vol %. As shown in Figure 7, the distillation rate in a stirred tank at 26 mbar and 5 °C reached a plateau of 10–12 vol % acetonitrile after 3 h. Even when the pressure was lowered to 10 mbar, the distillation rate slowed down significantly, and it would have taken >10 h to reach the target end point of 2 vol % acetonitrile. Therefore, the distillation was carried out at room temperature after the plateau was reached.²³ The ZI formation, filtration, and reconstitution were subsequently performed at 5 °C over 6–7 h. Isolation at 5 °C over a total of 9 h enabled the preparation of 5-g input batches of acceptable purity (Table 16).

By performing the ZI isolation at 5 °C, 10-g individual batches of API were isolated in laboratory-scale processing facilities (maximum vessel volume = 2.5 L) without degradation and in high purity (Table 17). Eventually, a total of 92 g of API were prepared.²⁴ Modified isolation techniques will be required to prepare >30-g batches because of the expected increase in hold times in the pilot-plant processing facilities that will be needed at

Table 15. Stability of the ZI solid versus temperature

sample	temp. (°C)	initial HPLC purity at 250 nm (AP)	final HPLC purity at 250 nm (AP)	stability ^a
1	22 ^b	96.9	95.3	<2 h
2	5 ^c	97.7	97.5	≥8 h
3	-20	96.4	95.8	<1 day
4	-70 ^d	96.4	97.3	1 day

^a Stability is defined as the time at which the HPLC purity of the material is 0.5 AP lower than its initial purity. ^b AP before ZI formation = 98.6. ^c AP after 24 h = 97.1. ^d AP after 2 days at -70 °C = 94.4.

Table 16. Processing time of the ZI isolation at 5 °C and room temperature (RT)

input of 3, temperature	processing time (h)						total isolation	estimated use of stability (%)
	distillation	ZI formation	ZI filtration	reconstitution	hold			
5 g at 5 °C/RT	1.5 (5 °C), 0.5 (RT) ^a	0.5	2.5 ^b	4.0 ^c	0.5	9.0 (5 °C), 0.5 (RT)	~60	
1.5 g at RT	4.0 ^d	1.0	1.3 ^e	1.0 ^f	0.0	7.3 (RT)	~210	

^a Distillation in rotary evaporator (initial volume = 1.8 L pooled fractions, 13–21 mbar, 0.5 vol % acetonitrile after distillation). ^b Filter diameter = 12 cm, two filters in parallel. ^c ZI reconstituted using overhead stirring. ^d Distillation in stirred tank (initial volume = 1.6 L pooled fractions, 22 mbar, 1.8 vol % acetonitrile after distillation). ^e Filter diameter = 9 cm. ^f ZI reconstituted using sonication.

these scales. We anticipate that a solution to overcome such limitations might be the development of a desalting procedure on a hydrophobic resin or via diafiltration. Similar techniques are currently in use for preparing commercial-scale quantities of other peptides. Our initial efforts focused on employing a hydrophobic resin (Amberchrom CG161S, polystyrene/divinylbenzene, 35 μm, 150 Å, Rohm and Haas). The pooled fractions were loaded on the resin ((load ≈ 5 g/L) and washed with 5 column volumes of water to remove the phosphate buffer. The API was then released from the resin using 25/75 vol % water/acetonitrile. The recovery was quantitative, the solution was concentrated by a factor of 2, and the water content was reduced by a factor of 3. After acetonitrile distillation, the API concentration was >10 mg/mL, meeting the desired target concentration.

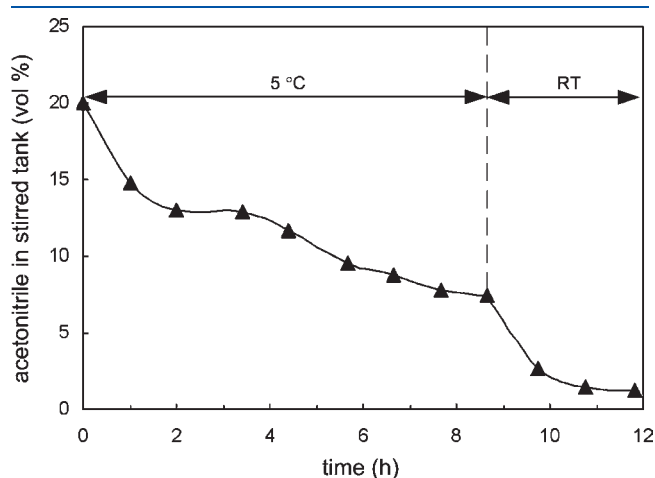


Figure 7. Acetonitrile distillation from 80/20 vol % 7 mM aqueous Na₂HPO₄, pH 7.2/acetonitrile in a stirred tank. Initial volume = 3.3 L. At 5 °C: distillation at 26 mbar for first 4 h and 10 mbar for next 4.5 h. At room temperature: distillation at 26 mbar for 3 h.

Table 17. Impurity profiles of API prepared via the ZI isolation at 5 °C

sample	HPLC purity at 250 nm (AP)						
	relative retention time (RRT) (–)						
	0.37	0.96	1.00	1.06	1.08	1.11	1.44
before distillation ^a	0.03	0.28	99.52	0.03	0.00	0.08	0.05
after distillation ^b	0.00	0.30	99.60	0.00	0.00	0.10	0.04
after isolation ^c	0.08	0.30	99.58	0.03	0.00	0.07	0.07
specification	0.79	0.50	97.0	0.65	0.50	0.50	0.73

^a One representative preparative injection. ^b One isolated subplot containing 12 g of API 1. ^c One batch containing 31 g of API 1.

CONCLUSION

In conclusion, we have described a synthetic process to prepare the peptidic epothilone–folic acid conjugate BMS-753493 in up to ~30-g batches. A robust chromatographic purification was developed by combining experimental studies with modeling. A batch-elution model was used to systematically optimize the purification method and to design the purification and isolation of API enriched with varying levels of an isomeric impurity. Isolation without significant degradation was conducted by converting the purified epothilone to a zwitterion and filtering to remove both buffer salts and water. This permitted us to avoid lyophilization in the preparation of bulk API. Upon reconstitution of the ZI solution and freezing at $-70\text{ }^{\circ}\text{C}$, the desired “frozen-solution” API was obtained. While the scalability of the process is limited by the stability of the ZI solid, the development of an alternate isolation strategy is under investigation.

EXPERIMENTAL SECTION

General Methods. The reaction progress was monitored on a Shimadzu LC-10AT HPLC instrument equipped with a Shimadzu SPD-10AV UV–vis detector. The HPLC method was run on a YMC Pack Pro C18, $3\text{ }\mu\text{m}$, $4.6\text{ mm} \times 50\text{ mm}$ column. The method conditions were mobile phase A, 100/0.05 vol % water/TFA; B, 100/0.05 vol % acetonitrile/TFA; gradient from 2% B to 90% B over 4 min; flow rate 3.0 mL/min; wavelength 278 nm. The retention times were 0.91 min (4), 1.69 min (2), 2.22 min (1), and 2.73 min (3). The reaction progress was monitored using the ratio of the areas of 1 to 2 because this HPLC method was not sensitive enough to detect traces of 3.

The impurities and degradants present in 1 were determined on a Waters Alliance 2695 HPLC instrument equipped with a Waters 2487 UV–vis detector. The HPLC method was run on a Waters XBridge BEH130 C18, $3.5\text{ }\mu\text{m}$, $4.6\text{ mm} \times 250\text{ mm}$ column. The method conditions were mobile phase A, 20 mM ammonium acetate in water, pH as is; B, 20 mM ammonium acetate in 15/85 vol % water/acetonitrile, pH as is; gradient from 1.5% B to 3.0% B over 8 min, followed by gradient from 3.0% B to 23.0% B over 12 min, isocratic at 23.0% B over 6.5 min, gradient from 23.0% B to 25.0% B over 3.5 min, isocratic at 25.0% B over 9 min, gradient from 25.0% B to 35.0% B over 5.5 min, gradient from 35.0% B to 36.0% B over 10 min, and gradient from 36.0% B to 100.0% B over 0.5 min; flow rate 1.0 mL/min; wavelength 250 nm; column temperature $30\text{ }^{\circ}\text{C}$; sample temperature $4\text{ }^{\circ}\text{C}$. The retention time was 37.00 min (1). The relative retention times were 0.96 (5) and 1.00 (1).

Reaction. Methanol (0.87 L) was degassed by purging with a vacuum/nitrogen manifold three times (degassing time per cycle = 5 min), and the epothilone 3 (19.7 g, 25 mmol corrected for potency) was charged to obtain a clear solution at $15\text{--}20\text{ }^{\circ}\text{C}$. A 352 mM aqueous solution of Na_2HPO_4 was prepared (50 g, final volume 1 L) and filtered through a $0.22\text{-}\mu\text{m}$ sterile PVDF filter (Durapore, Millipore). A 7 mM aqueous solution of Na_2HPO_4 was prepared (0.99 g, final volume 1 L), its pH was adjusted to 6.4 using 85 wt % H_3PO_4 (1.1 mL), and the resulting solution was filtered through another $0.22\text{-}\mu\text{m}$ sterile PVDF filter (Durapore). The peptide 2 (29.2 g, 29 mmol corrected for potency, 1.15 equiv) was suspended in water for injection (WFI, 0.87 L) at room temperature. A portion of the 352 mM Na_2HPO_4 solution (0.30 L) was added until the peptide was fully dissolved (pH 5.9).

The solution of 2 was degassed by purging with a vacuum/nitrogen manifold three times (degassing time per cycle = 5 min) and was added to the solution of 3 over 15 min at $15\text{--}20\text{ }^{\circ}\text{C}$. The reaction mixture was stirred, and the reaction progress was monitored via HPLC. At a reaction time of 3 h, the reaction was quenched with a portion of the 7 mM aqueous Na_2HPO_4 , pH 6.4 (0.72 L). The pH of the mixture was adjusted from pH 6.6 to 6.3 using 0.1 N HCl (0.1 L). The reaction mixture was passed through a $1\text{-}\mu\text{m}$ nylon filter (Nylasorb, Pall) followed by a $0.45\text{-}\mu\text{m}$ nylon filter (Nylaflor, Pall) to obtain a clear yellow solution, and was stored at $-70\text{ }^{\circ}\text{C}$.²⁵

Chromatographic Purification. A solution of Na_2HPO_4 (20 g) in WFI (20.00 kg) was adjusted to pH 7.2 using 85 wt % H_3PO_4 (34 g), and the solution was passed through a $0.22\text{-}\mu\text{m}$ sterile PVDF filter (Durapore). Acetonitrile (1.75 kg) was charged at room temperature and stirred for 10 min to produce mobile phase A' (10 vol % acetonitrile). The reaction crude was held at $4\text{ }^{\circ}\text{C}$ over <8 h and purified at room temperature, i.e., the mobile phases and column were kept at room temperature, by batch preparative reverse-phase HPLC using a 8 cm \times 30 cm DAC column (Novasep Prochrom LC80) packed with Amberchrom HPR10 (Rohm and Haas) and $2\text{-}\mu\text{m}$ frits (7,800–11,200 plates at 75 mL/min), an HPLC pumping system (Knauer, WellChrom preparative HPLC pump K-1800, 1 L/min pump heads, maximum discharge pressure of 75 bar up to 350 mL/min), and the initial purification method (10–50% B in 30 min, where A = 7 mM aqueous Na_2HPO_4 , pH 7.2, and B = acetonitrile; 132 mL/min). Injection volumes of 100–250 mL and loads of up to 2.1 g/L (3.1 g BMS-753493) were used. Mixed fractions enriched with the impurity 5 (3.0–12.0 AP) were purified using the model-based purification method (9.3–20.8% acetonitrile^{18,26} in 90 min, 132 mL/min) and a load of 3.8 g/L. After every injection the column was flushed (95 vol % acetonitrile, three column volumes) and equilibrated at the initial composition of either gradient (three column volumes). The eluted BMS-753493 peak was divided into 8 fractions and analyzed for HPLC purity. Fractions were selected and pooled to maximize the purification yield while meeting the purity specifications. Fractions were stored at $-70\text{ }^{\circ}\text{C}$ until the purification was complete.²⁷

The 8 cm \times 30 cm column was back flushed briefly (30 mL/min, 0.15 column volumes, 5/95 vol % buffer/acetonitrile) after every four injections to prevent the obstruction of the frits. Bioburden and endotoxin in the buffer solutions were controlled by using mixtures of 90/10 vol % buffer/acetonitrile as mobile phase A' and preparing fresh solutions daily. Adding 10 vol % acetonitrile to the buffer suppressed bioburden and endotoxin for at least 72 h. In contrast, bioburden (3 cfu/mL) was detected in the buffer (not mixed with acetonitrile) after 24 h. The initial purification method was thus run as 0–44% B in 30 min using A' and B = acetonitrile. For cleaning and depyrogenating the resin in place, 10/90 vol % 0.5 N aqueous NaOH/acetonitrile was used.

Isolation. The batch was split into three sublots for isolation. The isolation procedure for one subplot (11 g API) was as follows. The pooled fractions were distilled under vacuum (2 mbar and rotavapor bath temperature of $5\text{ }^{\circ}\text{C}$ for 1.5 h followed by 4 mbar and $19\text{ }^{\circ}\text{C}$ for 30 min, residual acetonitrile 0.4 vol %).²⁸ The pH of the fractions after distillation (pH 6.7) was adjusted to 4.3 at $5\text{ }^{\circ}\text{C}$ by adding 1 N HCl (30 mL). A yellow slurry was obtained. The slurry was collected via filtration ($1.0\text{ }\mu\text{m}$ nylon) at $5\text{ }^{\circ}\text{C}$ (diameter = 12 cm, two filters in parallel, 2.5 h). The ZI solid

was washed with WFI (68 mL) and dried under house vacuum (30 min). The ZI solid was resuspended in water at 5 °C (440 mL) and redissolved by adding 0.1 N NaOH (194 mL) over 4 h to pH 7.0 to afford a clear yellow solution (14.9 g/L) containing 10.6 g of **1**. The reconstituted solutions from the three sublots were pooled and diluted at 5 °C using WFI (370 mL). The pH of the diluted solution (pH 6.8) was adjusted to 7.0 using 0.1 N NaOH (17 mL). 31.1 g of **1** were obtained in a clear yellow solution (12.9 mg/mL, 99.6% HPLC AP, 79% yield, endotoxin BET <2.7 EU/mg). The final API solution was passed through a 0.22- μ m sterile PVDF filter (Durapore), transferred to polycarbonate containers, and frozen at -70 °C.

Analytical Characterization. No melting point endotherm was observed in the differential scanning calorimetry thermogram of the solid (amorphous). ¹H NMR (600 MHz, D₂O/CD₃CN (3.4:1.0), 25 °C) δ 8.57 (s, 1H), 7.55 (br d, *J* = 6.9 Hz, 2H), 7.08 (s, 1H), 6.56 (br d, *J* = 6.9 Hz, 2H), 6.42 (s, 1H), 5.11 (br d, *J* = 7.6 Hz, 1H), 4.67 (m, 1H), 4.57 (t, *J* = 6.2 Hz, 1H), 4.38 (m, 2H), 4.37 (m, 1H), 4.30 (m, 1H), 4.27 (m, 2H), 4.22 (m, 2H), 4.02 (m, 1H), 3.58 (br d, *J* = 7.9 Hz, 1H), 3.16 (m, 1H), 3.14 (m, 1H), 3.05 (m, 2H), 2.93 (m, 1H), 2.83 (m, 2H), 2.72 (m, 1H), 2.70 (m, 1H), 2.64 (m, 1H), 2.57 (s, 3H), 2.56 (m, 1H), 2.52 (m, 1H), 2.38 (m, 2H), 2.14 (m, 1H), 2.09 (m, 1H), 2.02 (m, 1H), 1.86 (s, 3H), 1.81 (m, 1H), 1.71 (m, 1H), 1.70 (m, 1H), 1.69 (m, 1H), 1.57 (m, 1H), 1.55 (m, 1H), 1.39 (m, 1H), 1.28 (s, 3H), 1.26 (m, 1H), 1.24 (m, 1H), 1.22 (m, 1H), 1.16 (m, 1H), 1.10 (d, *J* = 5.2 Hz, 3H), 1.00 (m, 1H), 0.93 (s, 3H), 0.90 (d, *J* = 3.8 Hz, 3H); ¹³C NMR (400 MHz, D₂O/CD₃CN (3.4:1.0), 25 °C): 221.9, 178.8, 178.1, 178.0, 176.4, 175.9, 174.1, 173.3, 172.9, 169.1, 167.5, 164.7, 157.2, 155.8, 155.0, 154.3, 151.3, 151.2, 149.7, 149.5, 139.4, 129.5, 127.7, 121.8, 119.9, 117.6, 112.6, 79.7, 77.3, 71.5, 68.1, 66.4, 57.0, 55.6, 54.8, 54.0, 53.7, 52.1, 46.1, 45.8, 43.8, 41.4, 41.3, 39.3, 39.1, 36.8, 36.1, 32.9, 31.7, 29.7, 29.2, 28.7, 27.3, 25.2, 24.8, 22.9, 19.6, 18.5, 18.1, 16.5, 14.9. MS (ESI) *m/z*: 1569.6 [M + H]⁺.

ASSOCIATED CONTENT

Supporting Information. This material is available free of charge via the Internet at <http://pubs.acs.org>.

AUTHOR INFORMATION

Corresponding Authors

*(S.-H.K.) Telephone: +1-609-818-6270. E-mail: soonghoon.kim@bms.com; (N. de M.) Telephone: +1-774-759-8404. E-mail: nuria.demas@lonza.com

Present Addresses

♦Cardiovascular Diseases Discovery Chemistry, 311 Pennington-Rocky Hill Road, Pennington, New Jersey 08534, United States

●Lonza Biologics Inc., 97 South Street, Hopkinton, Massachusetts 01748, United States

□BASF Custom Synthesis, 100 Campus Drive, Florham Park, New Jersey 07932, United States

■Zhejiang Apelo Kangyu Pharmaceutical Co. Ltd., 333 Jiangnan Road, Hengdian, Dongyang, Zhejiang, China

△Boehringer Ingelheim Pharmaceuticals Inc., 900 Ridgebury Road, Ridgefield, Connecticut 06877, United States

▲Pfizer Global Research and Development, Eastern Point Road, Groton, Connecticut 06340, United States

○Phenomenex Inc., 411 Madrid Avenue, Torrance, California 90501, United States

ACKNOWLEDGMENT

We thank Doris C. Chen, Robert P. Discordia, and Jaan A. Pesti for critical reading of the manuscript.

REFERENCES

- (1) Low, P. S.; Henne, W. A.; Doorneweerd, D. D. *Acc. Chem. Res.* **2008**, *41* (1), 120–129.
- (2) (a) Ladino, C. A.; Chari, R. V. J.; Bourret, L. A.; Kedersha, N. L.; Goldmacher, V. S. *Int. J. Cancer* **1997**, *73*, 859–864. (b) Leamon, C. P. *Curr. Opin. Invest. Drugs* **2008**, *9* (12), 1277–1286.
- (3) Vlahov, I. R.; Vite, G. D.; Kleindl, P. J.; Wang, Y.; Santhapuram, H. K. R.; You, F.; Howard, S. J.; Kim, S.-H.; Lee, F. Y.; Leamon, C. P. *Bioorg. Med. Chem. Lett.* **2010**, *20*, 4578–4581.
- (4) Feyen, F.; Cachoux, F.; Gertsch, J.; Wartmann, M.; Altmann, K.-H. *Acc. Chem. Res.* **2008**, *41* (1), 21–31.
- (5) (a) Vlahov, I. R.; Santhapuram, H. K. R.; Kleindl, P. J.; Howard, S. J.; Stanford, K. M.; Leamon, C. P. *Bioorg. Med. Chem. Lett.* **2006**, *16*, 5093–5096. (b) Reddy, J. A.; Dorton, R.; Westrick, E.; Dawson, A.; Smith, T.; Xu, L.-C.; Vetzal, M.; Kleindl, P.; Vlahov, I. R.; Leamon, C. P. *Cancer Res.* **2007**, *67* (9), 4434–4442. (c) Leamon, C. P.; Reddy, J. A.; Vlahov, I. R.; Westrick, E.; Parker, N.; Nicoson, J. S.; Vetzal, M. *Int. J. Cancer* **2007**, *121*, 1585–1592.
- (6) (a) Schneider, S. E.; Bray, B. L.; Mader, C. J.; Friedrich, P. E.; Anderson, M. W.; Taylor, T. S.; Boshernitzan, N.; Niemi, T. E.; Fulcher, B. C.; Whight, S. R.; White, J. M.; Greene, R. J.; Stoltenberg, L. E.; Lichty, M. J. *Pept. Sci.* **2005**, *11* (11), 744–753. (b) Andersson, L.; Blomberg, L.; Flegel, M.; Lepsa, L.; Nilsson, B.; Verlander, M. *Biopolymers: Pept. Science* **2000**, *55* (3), 227–250. (c) Bray, B. L. *Nat. Rev. Drug Discovery* **2003**, *2* (7), 587–593.
- (7) Vite, G. D.; Lee, F. Y.; Leamon, C. P.; Vlahov, I. R. Aziridinyl-epothilone compounds. WO 2007/140297 A2, 2007.
- (8) The stability of API solutions at pH 6.0 was at least comparable to that at pH 7.0.
- (9) Leamon, C. P. Personal communication, 2006.
- (10) A decontamination solution was developed to treat processing equipment. It was validated using a cell-based assay that measured residual cytotoxicity after deactivation.
- (11) Peptide **2** was synthesized by solid-phase synthesis starting from H-Cys(4-methoxytrityl)-2-chlorotrityl-resin using Fmoc-protected aminoacids and PyBOP and met the following specifications: HPLC purity \geq 95.0%, water content \leq 10.0 wt %. Detailed experimental conditions for the syntheses of **2** and **3** have been disclosed in ref 7.
- (12) A = 7 mM aqueous Na₂HPO₄, pH 7.2; B = acetonitrile.
- (13) Using a 0.39 cm \times 30 cm Nova-Pak HR C18 column (6 μ m, 60 Å, Waters), the retention times of API **1** were 12.4 min (gradient 10–50% B in 30 min), 8.3 min (82/18 vol % A/B), 19.0 min (84/16 vol % A/B), and >55 min (86/14 vol % A/B) at 1 mL/min.
- (14) About 2% of the API remained adsorbed on the resin and was desorbed in the flush step (5/95 vol % A/B) to regenerate the resin for the subsequent chromatographic cycle.
- (15) Mixed fractions of API (22.9 g) enriched with **5** (0.5–30 AP) were available from four batches in 143 bottles. Volumes = 13–211 mL, [API] = 0.2–11.7 mg/mL, \sim 20 vol % acetonitrile. Fractions from one batch required a rework (10 kDa ultrafiltration) to remove endotoxin prior to chromatographic purification.
- (16) Guiochon, G.; Felinger, A.; Shirazi, D. G.; Katti, A. M. *Fundamentals of Preparative and Nonlinear Chromatography*, 2nd ed.; Elsevier Academic Press: San Diego, CA, 2006.
- (17) Most of these experiments were carried out with relatively low loads of API (0.6–2.0 g/L).
- (18) A system suitability test was performed to ensure the reliability of the gradient separations. This SST consisted of a single gradient API

elution under analytical (i.e., not overloaded) conditions. The expected retention time was calculated from the batch-elution model and the API adsorption isotherm. If an offset between the experimental and calculated retention times was observed, it was assumed to be systematic; thus, the initial and final compositions of the gradient were shifted equally (i.e., the original slope was maintained) to obtain the calculated retention time.

(19) Solubilities are >80 mg/mL at pH >6.5, >60 mg/mL at pH <2, and <0.3 mg/mL at pH ~4.

(20) The Na content in the final API solution was consistent with a buffer-free trisodium salt, i.e., no additional Na from NaCl or NaH₂PO₄/Na₂HPO₄ was found. The Na content of the intermediate ZI was not measured.

(21) Unoptimized chromatographic load used in development runs.

(22) Studies of water/acetonitrile distillation using a reaction vessel (22 °C jacket, 10–65 mbar) and rotary evaporator (30 °C bath, 30 mbar) starting from pooled fractions containing 20 vol % acetonitrile and ~1.6 mg/mL API indicated that distillation to remove water and achieve >4 mg/mL API was outside the API stability window for scales >10 g. On the other hand, the volume of acetonitrile to distill per gram of API was approximately inversely proportional to the load because the API elution volume during chromatographic purification was not a strong function of the load.

(23) The entire distillation was not performed at room temperature to minimize degradation. The stability of the pooled fractions at 22 °C is 8–10 h and at 5 °C is ≥24 h (Table 7). The first part of the distillation was implemented at 5 °C because the stability of the material at 5 °C was at least 3 times longer than at room temperature and the distillation time at room temperature was not 3 times shorter than at 5 °C (Table 16).

(24) The maximum reaction batch size ever run used 19.7 g of epothilone 3 and generated 31.1 g of isolated API 1. This batch was split into three lots for isolation. Larger reaction scales were not attempted because larger batches of 3 were not available. The reaction is only slightly exothermic; no scale-up issues are anticipated.

(25) API solids did not precipitate out from the reaction crude upon thawing.

(26) The lowest acetonitrile concentration in mobile phase A was 10 vol % to suppress bioburden and endotoxin.

(27) API solids did not precipitate out from the purified fractions upon thawing.

(28) The distillation time was shorter than in development because of the lower pressure achieved in the cGMP processing facility and possibly an enhanced heat transfer coefficient in the rotavapor compared to that in the stirred tank.